PAPER

Efficient quantum simulation of open quantum system dynamics on noisy quantum computers

Physica Scripta

PAPER

Efficient quantum simulation of open quantum system dynamics on noisy quantum computers

Shin Sun[1], **Li-Chai Shih**[2] and **Yuan-Chung Cheng**[2,3,4]

[1] Experimental Quantum Information Physics Unit, Okinawa Institute of Science and Technology, Onna, Okinawa 904-0495, Japan
[2] Department of Chemistry, National Taiwan University, Taipei City 106, Taiwan
[3] Center for Quantum Science and Engineering, National Taiwan University, Taipei City 106, Taiwan
[4] Physics Division, National Center for Theoretical Sciences, Taipei City 106, Taiwan

E-mail: yuanchung@ntu.edu.tw

RECEIVED
13 September 2023

REVISED
21 December 2023

ACCEPTED FOR PUBLICATION
8 January 2024

PUBLISHED
1 February 2024

Keywords: quantum simulation, open quantum system, excitation energy transfer

Supplementary material for this article is available online

Abstract

Quantum simulation represents the most promising quantum application to demonstrate quantum advantage on near-term noisy intermediate-scale quantum (NISQ) computers, yet available quantum simulation algorithms are prone to errors and thus difficult to realize with limited circuit depth on nowadays quantum devices. Herein, we propose a novel scheme to utilize intrinsic gate errors of NISQ devices to enable controllable simulation of open quantum system dynamics without ancillary qubits or explicit bath engineering, thus turning unwanted quantum noises into useful quantum resources. Specifically, we simulate the energy transfer process in a photosynthetic dimer system on IBM-Q cloud. By employing tailored decoherence-inducing gates, we show that quantum dissipative dynamics can be simulated efficiently across coherent-to-incoherent regimes with results comparable to those of the numerically exact classical method. Moreover, we demonstrate a calibration routine that enables consistent and predictive simulations of open-quantum system dynamics in the intermediate coupling regime. This work provides a new direction for quantum advantage in the NISQ era.

1. Introduction

Quantum computers promise revolutionary advantages in simulating quantum systems highly important in physics and chemistry [1]. The concept of quantum simulation refers to utilizing quantum computers to simulate other quantum systems of interest with resources much smaller than those required for the same simulation in classical computers, and it could lead to significant breakthroughs in scientific research [2, 3]. Quantum simulation also represents one of the most critical and successful applications of near-term quantum computers [4]. However, although various quantum simulation algorithms have been proposed [5–9], many of them have limited practical advantages over the classical counterparts due to severe hardware constraints of current quantum devices. Contemporary quantum computers are prototypical noisy intermediate scale quantum (NISQ) devices [10, 11], as they are subjected to various coherent and decoherent noises as well as limited in size and connectivity.

Since fault-tolerant universal quantum computation [12, 13] is unlikely to be available in the near future, we are urged to find problems which are hard to solve on classical computers but suitable for NISQ computers in order to demonstrate quantum advantages for solving real-world problems. The simulation of open quantum systems is one of such problems with significant applications, as dissipative dynamics of open quantum systems [14, 15] play crucial roles in a broad range of physical and chemical phenomena of complex systems, such as photosynthetic light harvesting [16–18], and electron transfer in organic materials [19, 20]. Open quantum systems also stand at the brink of quantum to classical transition, which is of great importance for the

Table 1. Comparison of existing proposals for simulating open quantum systems on quantum computers.

	Platform	Ancillary qubits	Explicit bath engineering	Noise source
Maniscalco *et al* [29]	Trapped-ion	No	Yes	Reservoir engineering
Mostame *et al* [26]	Superconducting circuit	No	Yes	Qubit-resonator coupling
García-Pérez *et al* [28]	Superconducting circuit	Yes	No	Ancillary qubits
Wang *et al* [32]	NMR	No	Yes	Stochastically-modulated field
Rost *et al* [35]	Superconducting circuit	No	No	Idle operation
Tolunay *et al* [36]	Superconducting circuit	No	No	Idle operation
Guimarães *et al* [37]	Superconducting circuit	No	No	Transoformed gate error
Sun *et al* (This work)	Superconducting circuit	No	No	Decoherence-inducing gates

fundamentals of the quantum theory [21]. Hence, enabling efficient and accurate simulation of open quantum system dynamics could lead to significant advances in both quantum science and technology.

Conventional methods for the simulation of open quantum system dynamics on classical computers, such as the quantum master equation approach [14], are based on certain weak-coupling assumptions about the underlying system-bath interactions. When the assumptions do not hold, non-perturbative treatments such as the numerically exact hierarchical equation of motion (HEOM) method [22–25] become necessary in order to yield accurate results. However, these exact methods on classical computers exhibit extremely steep scaling against the accuracy and system size, which hinders our understanding of the dynamical behaviors of complex open quantum systems.

On the other hand, there exist several proposals for simulating open quantum system on quantum computers [26–35]. Most of the previous studies focused on theories and algorithms. For example, Maniscalco *et al* [29] proposed to simulate the quantum Brownian motion by engineering an artificial reservoir coupled to a single trapped ion, and Aspuru-Guzik and coworkers [26] proposed an superconducting analog open quantum simulator for Fenna-Matthews-Olson complex, where the required system-bath interactions are introduced though explicit engineering of qubit-resonator couplings. Experimental realizations of quantum simulation of open-quantum system dynamics on NISQ systems remain largely unexplored. Recently, García-Pérez *et al* [28] simulated various decoherence channels on superconducting quantum computers by explicitly realizing the non-unitary dynamics with ancillary qubits. Moreover, Wang *et al* [32] utilized a NMR quantum computer to simulate photosynthetic systems with the dephasing noises generated by stochastically-modulated control fields. To our knowledge, the four-qubit photosynthetic system they simulated remains the largest open quantum system simulated on a quantum computer. Nevertheless, due to the necessity of either precise multi-qubit control or explicit system-bath engineering with ancillary qubits, the resources overheads needed for these previously published quantum simulation algorithms for open-quantum systems are still formidable for nowadays NISQ quantum devices. We also noted that there are several recent works focusing on a similar approach to ours to simulate open quantum systems with noisy quantum devices. However, the controlling of noise strengths is different from the approach used by us. In [35, 36], the dissipative dynamics of radical pairs is simulated via the insertion of identity gates and spin-echo pulses. In [37], an excitation energy transfer dynamics of a linear chain of molecules is simulated using randomized compiling to transform the intrinsic noises. Our approach emphasizes implementing decoherence-inducing gate sequences to achieve controllable simulation of open quantum system dynamics, and we also demonstrate the usage of several distinctive gate sequences. We summarize the existing proposals in table 1.

Let us recall Feynman in his famous quote [38]:

> 'Nature isn't classical, dammit, and if you want to make a simulation of nature, you'd better make it quantum mechanical, and by golly it's a wonderful problem, because it doesn't look so easy.'

In the same spirit, we might as well simulate dissipative quantum dynamics using intrinsic noises in quantum computers. In this work, we propose to simulate open quantum system dynamics on quantum computers by directly exploiting the errors generated on the gate level in superconducting NISQ devices, which is an idea that strongly differs from existing proposals. The idea of utilizing decoherence and thermal effects in quantum computers to simulate quantum dynamics was previously suggested by Lloyd and coworkers [39], but the implementation is still an ongoing research area. For most quantum algorithms, quantum noises are undesirable and destructive. Nevertheless, we recognize that the decoherence effects induced by quantum noises are necessary and can be used as resources for simulations of open quantum systems. Our approach thus does not require explicit engineering of the control field, and no extra qubits for modeling the environment are needed either.

In this paper, we demonstrate that gate errors on IBM-Q cloud quantum computers can be controlled and utilized to simulate excitation energy transfer (EET) dynamics in a molecular exciton dimer system under tunable dissipative environments, and we compare the simulation results with HEOM calculations to validate that they correspond to dynamics induced by realistic system-bath interactions. We also show that quantum computers can quantitatively predict quantum dissipative dynamics at the intermediate system-bath coupling regimes that are hard to simulate accurately with classical methods. Moreover, since the device instability for both qubit and quantum gates are still high for NISQ computers [40, 41], we demonstrate designed calibration routines for noise strengths to achieve consistent simulations. In summary, our approach shows the possibility of utilizing NISQ devices as quantum noise generators as well as embracing the noises to simulate physical systems. This opens new directions for the simulation of open quantum system dynamics and various stochastic systems such as in biology, finance, or cryptography.

2. Quantum simulation of coherent energy transfer

2.1. Exciton model

To demonstrate the simulation of open quantum system dynamics on noisy quantum computers, we adopt a simple exciton model that describes EET in photosynthetic systems. In the model, physical systems are represented as different monomers called 'sites', which constitute the whole complex, and two quantum states, the ground state and the excited state, are considered for each site. This two-level property makes them mapped naturally to qubits, and thus ideal target systems to be simulated on quantum computers. The Hamiltonian describing an excitonic system with N sites in the second-quantized form is

$$H = \sum_{i=1}^{N} \epsilon_i a_i^{\dagger} a_i + \sum_{i \neq j=1}^{N} J_{ij} a_i^{\dagger} a_j \tag{1}$$

where $a_i^{\dagger}(a_i)$ is the creation (annihilation) operator acting on site i. It is convenient to introduce the state $|0\rangle$, which corresponds to the state with all sites in the ground state, and $|i\rangle = a_i^{\dagger}|0\rangle$, which corresponds to the state with a single excitation at site i while other sites are in the ground state. The diagonal matrix element ϵ_i is the site energy of $|i\rangle$, and the off-diagonal term J_{ij} corresponds to excitonic coupling between $|i\rangle$ and $|j\rangle$. For simplicity, we consider a symmetric dimer system ($N = 2, \epsilon_1 = \epsilon_2 = 0$) with excitonic coupling $J_{12} = J_0$. This model also corresponds to the spin-boson problem or the Heisenberg XY model for magnetism [42]. In this work, we specifically focus on the dynamics in the one-exciton manifold for EET.

2.2. Quantum circuit and simulated coherent dynamics

To represent and propagate the exciton dynamics efficiently on quantum computers, we encode the exciton occupancies of the dimer system in the computational basis of two qubits. The Hamiltonian of the system is mapped to Pauli operators acting on the qubit Hilbert space via a Jordan-Wigner type transformation, and the details of the encoding circuit are described in the Method section. Thus, the quantum circuit which simulates the system propagator e^{-iHt} ($\hbar = 1$) can be constructed as shown in figure 1(a), where θ corresponds to the simulation time. Note that the resulting circuit for the propagator is exact in the symmetric dimer case due to the commutativity of the two terms in the system Hamiltonian. More generally, one has to build the propagator through Trotterization or other efficient state propagation schemes [43] for a general biased excitonic system. To retrieve the dynamical population information, we perform projective measurements in the qubit computational basis, and renormalize the probabilities within the one-exciton manifold (see Methods) to compensate the leakage errors.

We experimentally simulated the time evolution of the dimer system with initial population on site 1 using the quantum circuit depicted in figure 1(a) on the IBM-Q superconducting quantum computers [44]. Figure 2 depicts the simulated population dynamics. The results show a perfect coherent Rabi oscillation ('quantum beating'). This validates the mapping and confirms that our renormalization procedure to account for the leakage error does not affect the coherence in the one-exciton manifold. Also, this result demonstrated that the unitary propagator for our model system is not too noisy and could produce correct coherent dynamics.

3. Tailored decoherence-inducing gates

3.1. Decoherence engineering by prepending identity gate sequences

To simulate realistic energy transfer dynamics on IBM-Q systems, we aim to utilize intrinsic imperfections in the quantum gates to model a dissipative environment in a controllable manner. To this end, we prepend a dissipation part to the simulation circuit by a number of gate sequences that ideally contract to the identity gate (figure 1(b)). Due to the gate errors, the identity gate sequences will introduce quantum noise into the simulation

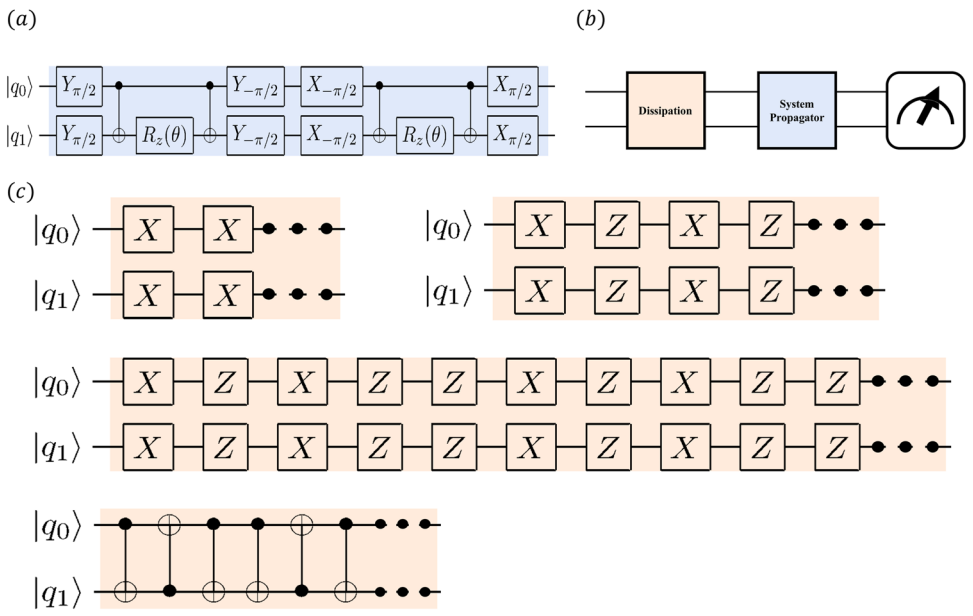

Figure 1. Quantum circuits for the dissipative quantum system simulation. (a) The circuit implementing the time-evolution propagator for the unbiased exciton dimer in our experiments. (b) Illustration of the simulation scheme. The full simulation circuit first undergoes dissipative operation via different decoherence-inducing gates that introduce decoherence into the simulated system and followed by the propagator of the system Hamiltonian. (c) Various decoherence-inducing gate sequences used for the dissipation circuit.

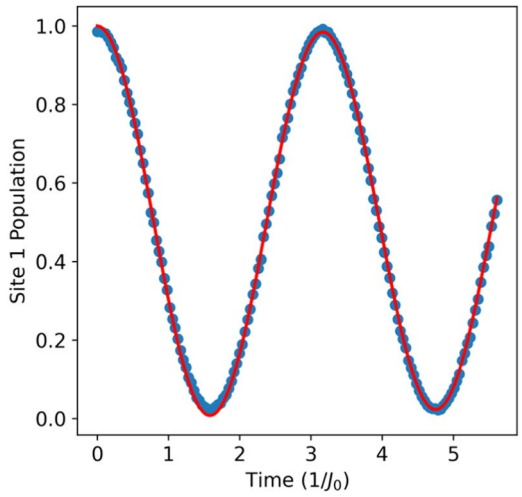

Figure 2. Simulated coherent dynamics of the dimer system. Population on site 1 as a function of time is depicted when the system is initially prepared as $|\psi(0)\rangle = |1\rangle$. The simulation result obtained on ibmq_bogota (blue dots) and a cosine function (red line) are both shown.

on NISQ devices. We thus refer to them as 'decoherence-inducing' gates in this work. The system propagator then changes the frame of the system from the interaction picture to Schrödinger picture at a given simulation time. Finally, projective measurements are performed to monitor site populations.

To tune the strength of system-bath couplings, we control the number of decoherence-inducing gates applied per unit simulation time. Therefore, we define a damping coefficient $d = \frac{N_I}{t/\Delta T_D}$, where t is the total simulation time, ΔT_D is the decoherence period, and N_I is the number of decoherence-inducing gates applied. The damping coefficient can then be adjusted in the quantum simulation to realize different system-bath coupling strengths.

Regarding decoherence-inducing gates, we examined four types of identity gate sequences as shown in figure 1(c), including 1.$(X)^2$ 2.$(XZ)^2$ 3.$(XZXZ)^2$ 4.$(SWAP)^2$. Gate sequences 1–3 act on a single qubit, while gate 4 is a non-local gate. These gate sequences are chosen based on a series of tomography studies on noisy qubit dynamics on the IBM-Q systems. To illustrate the characters of the noises induced by the aforementioned gate

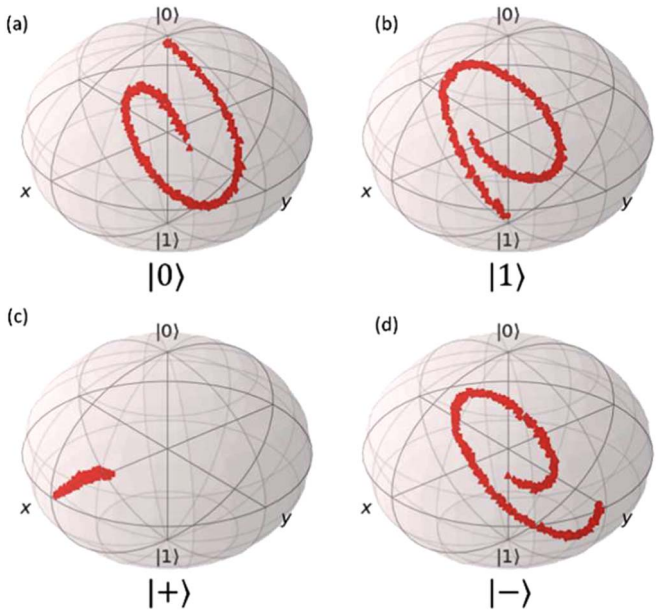

Figure 3. Bloch sphere dynamics induced by the $(X)^2$ gate on four different initial states: (a) $|0\rangle$, (b) $|1\rangle$, (c) $|+\rangle$, (d) $|-\rangle$. In the simulation, we initialize a qubit in the corresponding initial state, apply $(X)^2$ gates repeatedly by n time (n is between 0-300), and then perform quantum state tomography to obtain the Bloch vector of the qubit state after n $(X)^2$ operations. The Bloch vector is then depicted by a dot on a Bloch sphere, and the dot is traced continuously with an increasing number of applied gates. (a)-(d) all show the effect of rotating around the X axis and shortening towards the center.

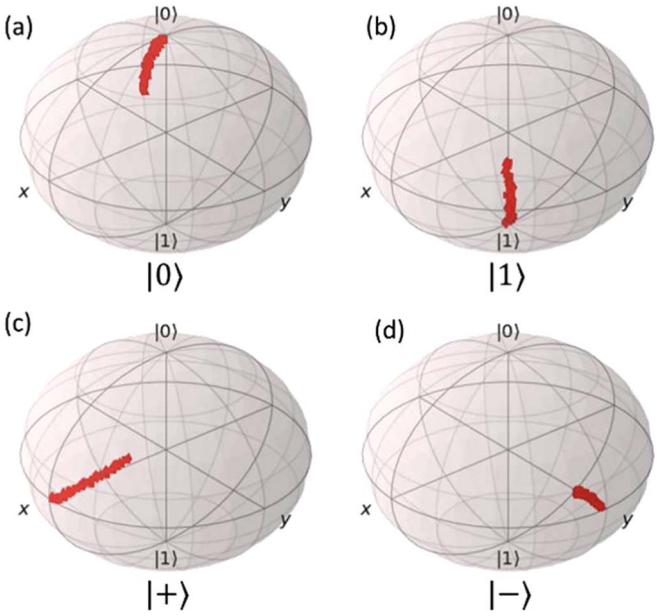

Figure 4. Bloch sphere dynamics induced by the $(XZ)^2$ gate. The results were obtained similarly as those presented in figure 3, except for that $(XZ)^2$ gates were applied repeatedly. In (a), a systematic rotation is still present.

sequences, we plot single qubit Bloch sphere dynamics induced by repeated operation of these gates and show the results in figure 3–5, respectively.

Figure 3 shows that the $(X)^2$ introduces a depolarization-type as well as a systematic coherent error (over-rotation), which does not mimic well-behaved random decoherence noises in a quantum system. In order to eliminate the drift in the X gate error and obtain more consistent random noises, we employ echo-type equivalents to the $(X)^2$ gate, the $(XZ)^2$ gate, and the corresponding higher order $(XZXZ)^2$ gate as the decoherence-inducing gates. The design of these gates is related to the compensating pulse sequence techniques [45] (see section S5 in the SI), which dynamically correct the X over-rotation. Due to the phase error, the $(XZ)^2$

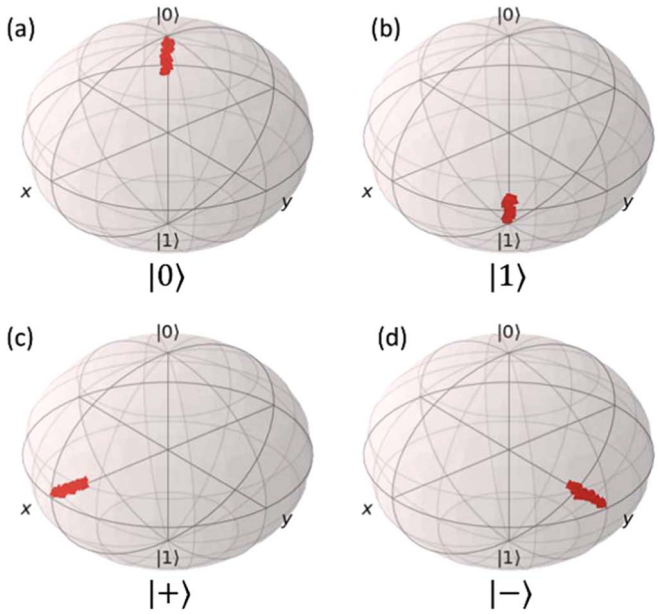

Figure 5. Bloch sphere dynamics induced by the $(XZXZZ)^2$ gate. The results were obtained similarly as those presented in figure 3, except for that $(XZXZZ)^2$ gates were applied repeatedly. The errors can be seen as a depolarization type error without systematic rotation.

does not remove the over-rotation completely. Nevertheless, the $(XZXZZ)^2$ sequence clearly induces a depolarization-like random noise, and it can thus be used to model a physical decoherence process.

It is interesting to note that the idea of using controlled coupling of a quantum system to its environment to engineer open-system dynamics has been realized previously. For instance, Barreiro *et al* [46] utilized dissipative quantum systems on trapped-ion architectures by combining multi-qubit gates and optical pumping techniques to prepare highly entangled quantum states. More recently, Rost *et al* [35] proposed a scheme for simulating open quantum systems by using intrinsic qubit noise. In their work, the decoherence effects are introduced to the quantum simulation via the 'idle' operation, which exhibits minimal overhead for simulating noises, but then the achievable bath conditions are solely determined by the intrinsic qubit properties. Our study indicates that the intrinsic qubit dissipation and gate errors could be complicated and can not be used for controlled open-system dynamics engineering. Therefore, in our proposed scheme, we shift the attention from imperfections in qubits to pulses, and this allows us to control the system-bath couplings in a much more flexible manner with pulse engineering. Consequently, our work significantly differs from previous methods in the design and implementation of the tailored decoherence-inducing gate sequences.

Finally, we note that because the virtual-Z gate implementation on IBMQ systems [47] corresponds to a mere frame shift of the subsequent pulses, it does not introduce a real time elapse in the simulation (i.e. no pulse is applied). Hence, Z gates cannot introduce gate noises. We therefore choose X gate as our primary decoherence-inducing single-qubit gate. In the following, we systematically analyze the dissipative dynamics induced by the four types of gate sequences, and details of the implementation and parameters used in this work are given in the Methods section.

3.2. Dissipative dynamics induced by single-qubit gate sequences

To investigate the effect of the coherent error on the simulation of population dynamics and the design of decoherence-inducing gate sequences, we first employ $(X)^2$ gates to simulate EET dynamics of the model dimer system. Figure 6 shows the simulated population dynamics at four different damping coefficients. At small damping coefficients ($d = 20$ and $d = 30$), the decoherence of the quantum beating is apparent and becomes more pronounced as d increases, which is in line with our proposal. However, at larger damping coefficients ($d = 50$ and $d = 70$), the population dynamics exhibit unphysical multifrequency behavior and large population revival; thus, the simulated dynamics cannot reach equilibrium and do not correspond to physical dissipative dynamics. These results indicate that $(X)^2$ does not introduce realistic decoherence effects into the EET dynamics and thus cannot be used as a proper decoherence-inducing gate.

The unrealistic dynamics is a consequence of the systematic drift in the noise, as shown in figure 3. Such coherent errors produce non-physical results in the EET simulation. In other words, applying $(X)^2$ gates results in the simulation of an effective Hamiltonian that is different from the target Hamiltonian. Thus, our idea of

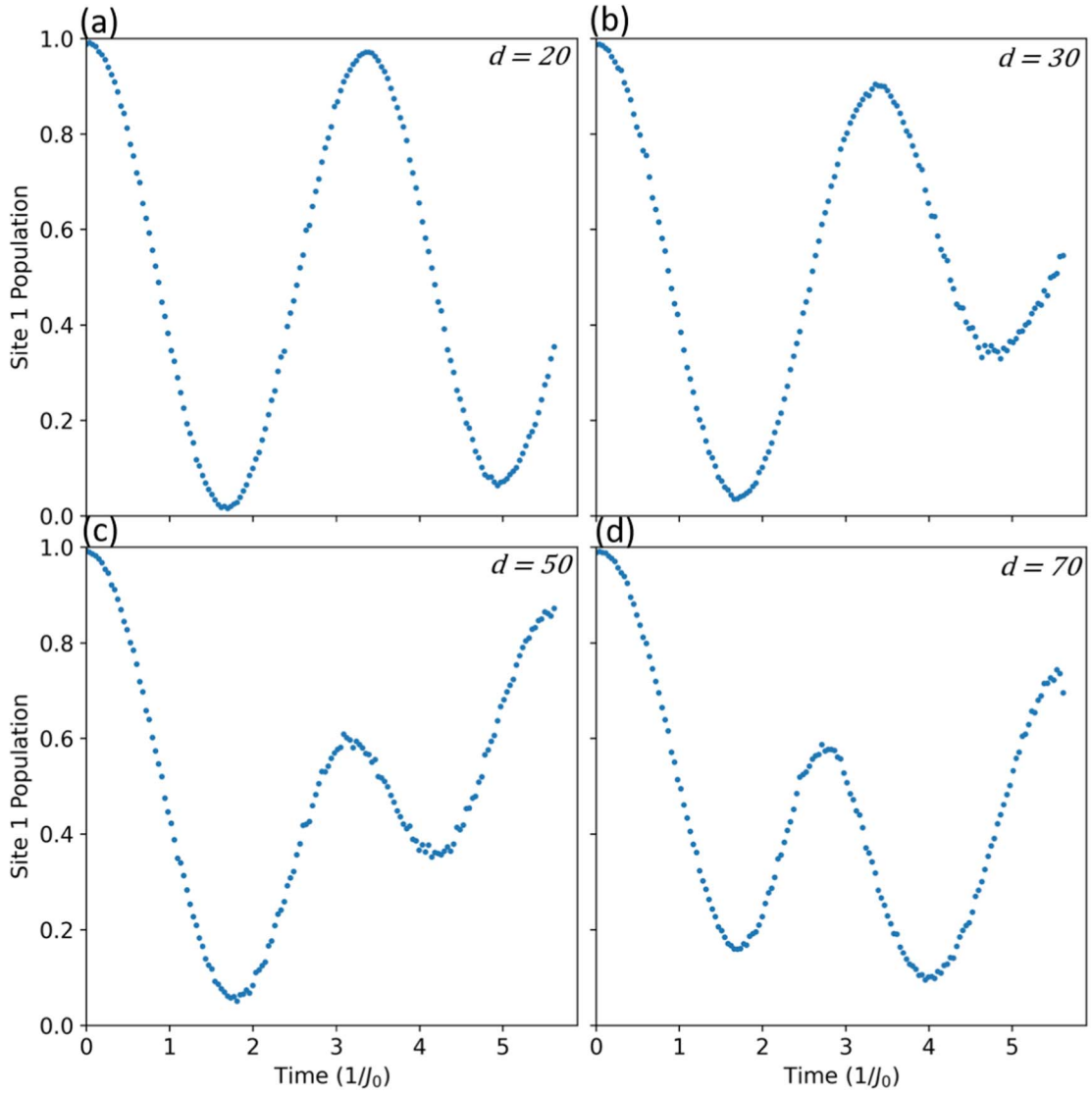

Figure 6. Simulated dissipative dynamics induced by $(X)^2$. We plot the population on site 1 (blue dots) as a function of time at 4 different damping coefficients. The decoherence effects are induced by applying the $(X)^2$ gates. (a) $d = 20$, (b) $d = 30$, (c) $d = 50$, and (d) $d = 70$. Experiments were performed on ibmq_bogota.

introducing identity gates to simulate noises in open quantum systems can not be realized by arbitrary identity gates. The decoherence-inducing gate sequences must be specifically designed. The issue could have been resolved by adding an offset to each X rotation to counteract the over-rotation, but the downside is that the over-rotation angle is then needed for each experiment beforehand, which is not practical given that the stabilities of the available quantum computers are still less than perfect.

We have shown that the over-rotation in the X gates on IBM-Q can be fixed by introducing echo-like gate sequence such as in $(XZXZ)^2$ gates (figure 5). Therefore, we employed $(XZXZ)^2$ as the decoherence-inducing gate, and assess the population dynamics for the EET process under different damping coefficients in the results shown in figure 7. The decoherence effect can be seen in the damping of the quantum beating, and the decay rate increases with the increase of the damping coefficient consistently. This confirms that the $(XZXZ)^2$ can be used as a decoherence-inducing gate sequence to introduce quantum noises into the simulation. However, even when the damping coefficient is large ($d = 35$, where the circuit depth is closed to the device limit), the population dynamics still remain coherent, and this restricts us from exploring the EET dynamics in the incoherent regime. Furthermore, the maximum time duration of the simulation is limited by the deepest circuit depth available on the NISQ devices. As d increases, the number of gates needed to perform simulation in a unit time also increases, which limits the available simulation time. Therefore, $(XZXZ)^2$ represents a decoherence-inducing gate sequence that is suitable for simulating quantum dynamics in the weak to intermediate system-bath coupling regime. For strong system-bath coupling systems, a more general decoherence-inducing gate sequence is still desirable.

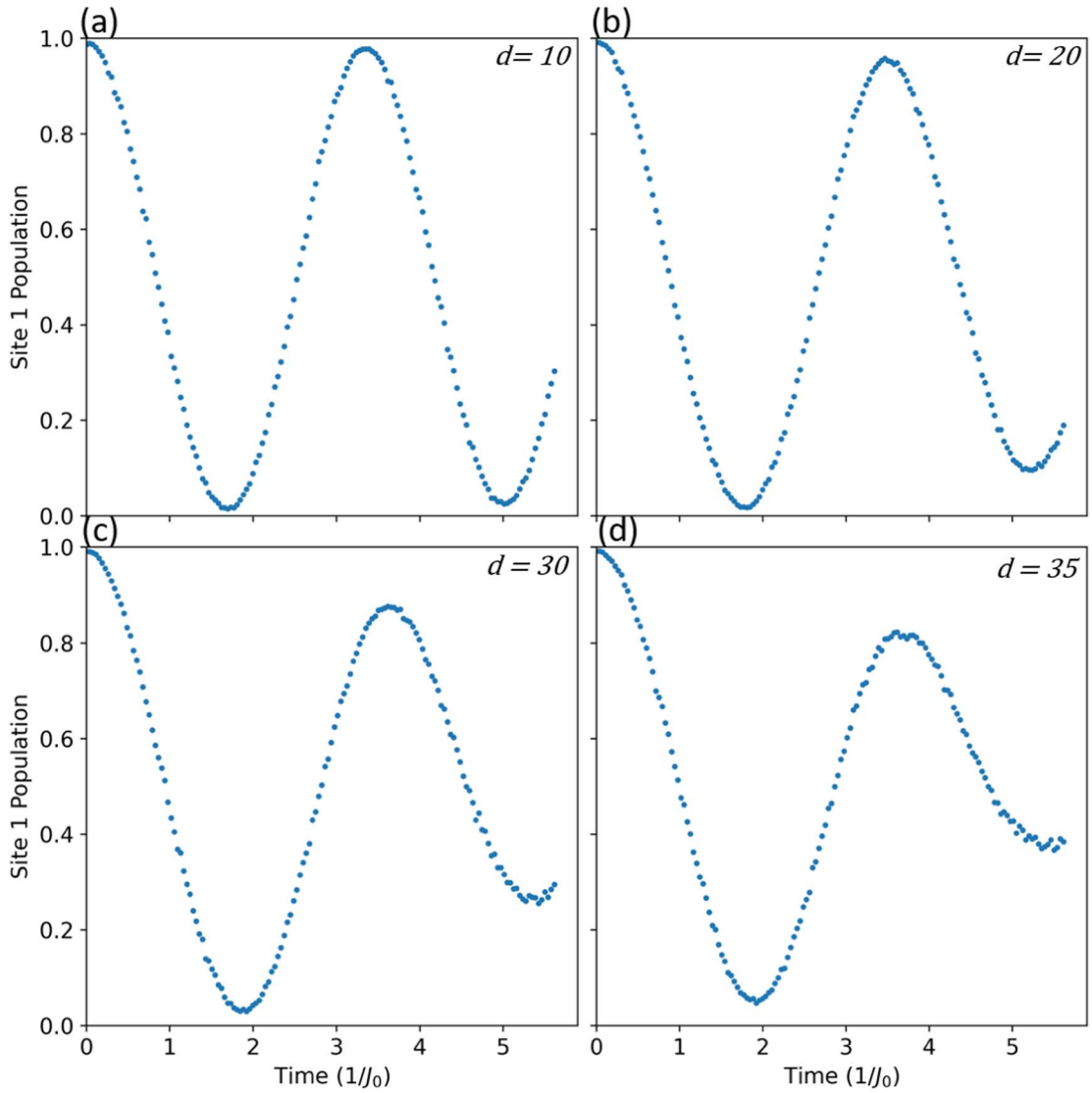

Figure 7. Simulated dissipative dynamics induced by $(XZXZZ)^2$. We plot the population dynamics on site 1 as a function of time under 4 different damping coefficients. The decoherence effects are induced by applying the $(XZXZZ)^2$ gates. (a) $d = 10$, (b) $d = 20$, (c) $d = 30$, and (d) $d = 35$. Experiments were performed on ibmq_bogota.

3.3. Dissipative dynamics under $(SWAP)^2$ gate sequences

In addition to single-qubit gates, two-qubit gates could also be utilized to construct decoherence-inducing gate sequences. We discovered that the non-local $(SWAP)^2$ gates on IBM-Q systems can introduce consistent decoherence effects into the model system and drive the system towards equilibrium efficiently. In figure 8, the population dynamics under $(SWAP)^2$ with different damping coefficients for the model system are depicted. The decay of the quantum beating is much faster compared to results shown in figure 7, suggesting that the noise introduced by the $(SWAP)^2$ gate is stronger than that introduced by the $(XZXZZ)^2$ gate. The system even exhibits incoherent transfer dynamics at a large d (figure 8(d)), which enables us to study the dissipative dynamics in the strong coupling regimes. Since the dissipative dynamics under $(SWAP)^2$ gates are consistent throughout coherent to incoherent regime, we quantitatively analyze and compare them to realistic open quantum system dynamics. The possibility of combining different types of gate sequences or other pulse-level techniques to achieve finer control over system-bath couplings is left for future research.

Furthermore, we extract the population transfer rate by fitting the dynamics at each damping coefficient with an exponential-cosine function, and plot the rates against the damping coefficients (figure 9). The relation between decay rate and damping coefficient varies under different system-bath coupling strengths. At weak system-bath couplings (small damping coefficients), the decay rate approximately increases linearly with respect to the damping coefficient ($d = 0$ to $d = 10$); however, as the damping coefficient further increases ($d > 10$), the rate exhibits a turnover behavior. It is interesting and important to note that the relation is not monotonic, suggesting an optimal transfer rate at the intermediate coupling regime in accordance with previous EET studies

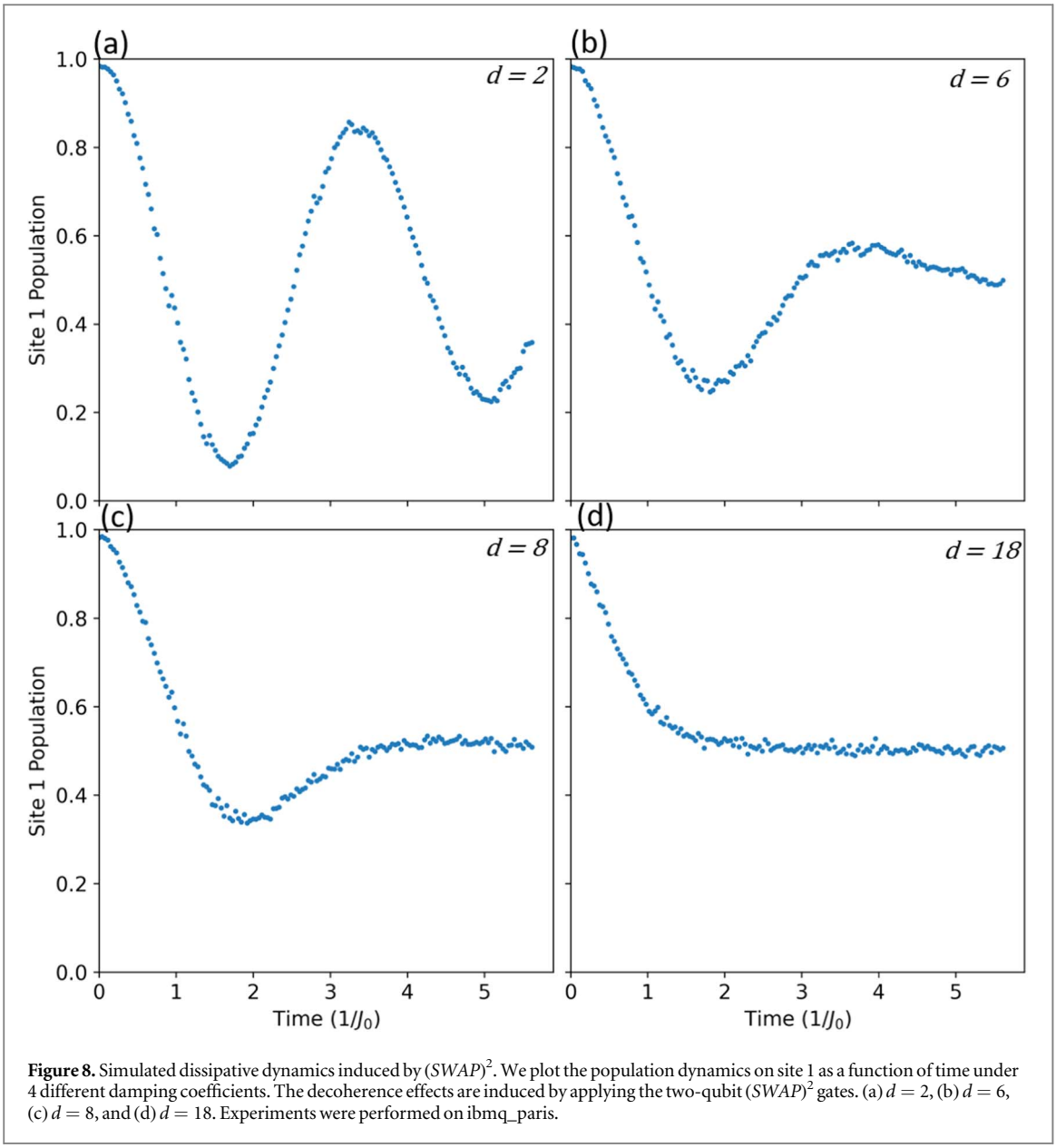

Figure 8. Simulated dissipative dynamics induced by $(SWAP)^2$. We plot the population dynamics on site 1 as a function of time under 4 different damping coefficients. The decoherence effects are induced by applying the two-qubit $(SWAP)^2$ gates. (a) $d = 2$, (b) $d = 6$, (c) $d = 8$, and (d) $d = 18$. Experiments were performed on ibmq_paris.

[24, 48, 49]. The behavior also suggests that our simulation results are non-trivial in the sense that they cannot be reproduced by simple Redfield-type theories. Note that the computational costs in terms of number of qubits and circuit depth needed in our proposed scheme are linear with respect to the number of sites (N) and simulation time (t), respectively. Moreover, the dissipative part can be introduced by using at most two-qubit gates that can be executed in parallel on nowadays superconducting quantum computers. Thus, the proposed scheme should be able to be easily scaled up to simulate open quantum system dynamics for multiple-site systems.

4. Validity of the method

4.1. Comparison with numerically exact heom simulations

To validate that our simulation based on $(SWAP)^2$ decoherence-inducing gate represents dynamics of a realistic open quantum system, we compare our results to those obtained by classical computation based on a microscopic modeling of system-bath interactions. To this end, we fit our quantum simulation data to those obtained from the hierarchical equation of motion using the Parallel Hierarchy equations of Motion Integrator program [50] on classical computers. The HEOM method employs a Drude-Lorentz type spectral density to model system-bath interactions:

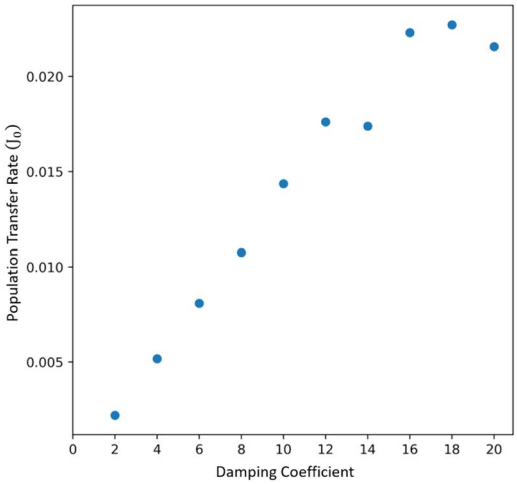

Figure 9. Simulated population transfer rate as a function of damping coefficient. Blue dots depict population transfer rate from $|1\rangle$ to $|2\rangle$ extracted from quantum simulation using $(SWAP)^2$ as decoherence-inducing gate sequence at different damping coefficients. Experiments were performed on ibmq_paris

$$J(\omega) = \frac{\lambda}{2}\frac{\gamma\omega}{\gamma^2 + \omega^2} \tag{2}$$

where λ is the reorganization energy, representing the system-bath coupling strength, and γ is the cut-off frequency that corresponds to the inverse bath relaxation time scale. HEOM has been recognized as a highly accurate method for EET dynamics; however, the full HEOM method requires solving a system of non-polynomial number of differential equations. As a result, HEOM calculations need truncation at a certain hierarchical level and exhibit extremely stiff computational cost against system size, making it best suited for small-size systems.

We choose to fit HEOM dynamics to the dynamics simulated using the $(SWAP)^2$ decoherence-inducing gates at two cases, a weak coupling case with $d = 2$ and a strong coupling case with $d = 18$. For the HEOM model parameters adopted in the fitting, we assume that each site in the dimer is coupled to identical and independent baths, and fix $J_0 = 100\ cm^{-1}$, $\gamma = 100\ ps^{-1}$, and the temperature at 300 K. We only vary λ in the HEOM model to reproduce the simulated dynamics using $(SWAP)^2$ gates on IBM-Q systems. In figure 10(a) and figure 10(b), we compare the population dynamics simulated on the IBMQ devices with the best HEOM fit for the $d = 2$ and $d = 18$ cases, respectively. The optimal HEOM parameters are listed in table 1. The results demonstrate that both coherent and incoherent EET dynamics simulated by the $(SWAP)^2$ decoherence-inducing gates on IBMQ devices can be quantitatively reproduced by microscopic HEOM calculations. Evidently, our proposed scheme can simulate realistic dissipative quantum dynamics with controllable system-bath coupling strengths.

Furthermore, the excellent agreement between dissipative dynamics induced by $(SWAP)^2$ gates and HEOM simulation of a microscopic model system provides crucial insights into the characteristics of the errors induced by the $(SWAP)^2$ gates. The Drude-Lorentz bath model adopted in the HEOM method represents an overdamped Brownian bath with Gaussian random fluctuations, and it should not be too surprising that the gate errors in IBM-Q systems could be quantitatively described by such a random process. In this regard, the fit to HEOM dynamics provides a consistent framework to extract error characteristics in quantum gates implemented in a quantum computer, as shown in the bath parameters listed in table 2. Such characteristics could be dependent on the type of decoherence-introducing gates as well as the hardware, and could have significant implications in optimizations of quantum algorithms and even designs of quantum error-correction schemes. This direction of research is a work in progress and will be reported in another paper.

Knowing that the simulation scheme has worked, we then investigate if we could use the scheme to predict the dissipative dynamics at other system-bath coupling strengths by controlling the damping coefficient. To this end, we assume a linear relationship between the damping coefficient and bath reorganization energy in the microscopic model. According to table 2, we can determine the required damping coefficient used in the quantum simulation for simulating dynamics with a given reorganization energy. For instance, a model system with $\lambda = 120\ \text{cm}^{-1}$ should correspond to the quantum simulation with $d = 10$. In figure 10(c), we plot the simulated dynamics at $d = 10$ and the HEOM result with $\lambda = 120\ \text{cm}^{-1}$. Note that there are no free parameters in both simulation shown here. The excellent agreement between them provides strong numerical evidence to support that the proposed scheme for dissipative quantum dynamics simulation can be used as a predictive tool, especially in the difficult intermediate coupling regime.

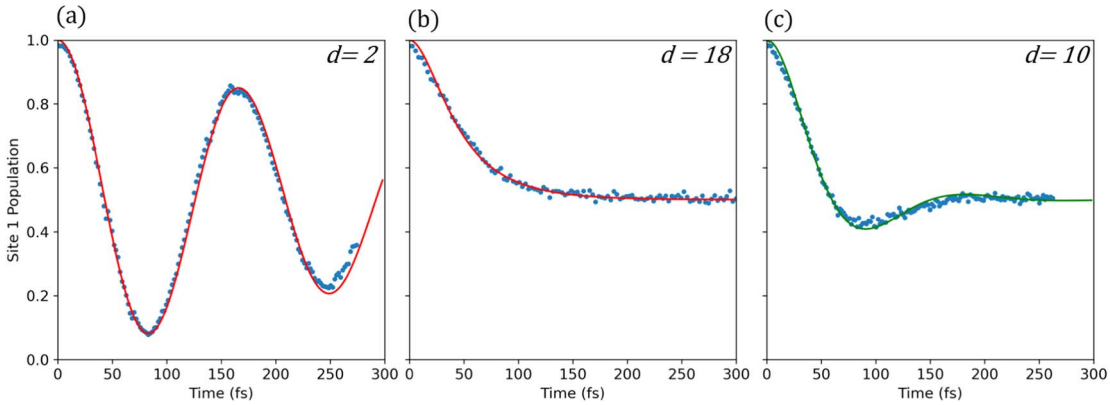

Figure 10. HEOM analysis of the simulated dynamics induced by $(SWAP)^2$ gates. The simulated population dynamics at three system-bath coupling parameters are shown: (a) weak coupling ($d = 2$), (b) strong coupling ($d = 18$), and (c) intermediate coupling ($d = 10$). The weak- and strong-coupling results are fitted individually with HEOM simulations, of which the results are shown as red lines and the fitting parameters are listed in table 1. With the fitted data, we assume a linear relationship between the reorganization energy and damping coefficient, and use quantum simulation to predict the dynamics at $\lambda = 120$ cm^{-1}. The predicted dynamics and the corresponding HEOM dynamics are shown as dots and the green line, respectively, in (c).

Table 2. The fitted HEOM parameters for the dissipative dynamics shown in figure 10.

	Underdamped	Overdamped
Damping coefficient	2	18
Excitonic coupling	100 cm^{-1}	100 cm^{-1}
Cutoff frequency	100 ps^{-1}	100 ps^{-1}
Reorganization energy	15 cm^{-1}	227 cm^{-1}
Hierarchy truncation	8	8
Temperature	300 K	300 K

4.2. Temporal stability and calibration scheme

During our study, we also found that the gate noises on IBM-Q superconducting devices in general could vary on a daily basis (see section S4 in the SI). Therefore, it is crucial that we assess the stability of our scheme on different days. We thus performed on different days a series of simulations of the EET dynamics using $(SWAP)^2$ gates with different damping coefficients, and for each damping coefficient, we fit the simulated population dynamics with HEOM calculations to analyze the relationship between the fitted reorganization energies and damping coefficients. In figure 11, we plot the calibration curves of the fitted reorganization energies against the damping coefficients for two separate sets of simulations executed on different days. We observe that the two curves remain linear, yet their slopes are different, which indicates that the device shows different levels of noise strength on different days, and it could affect our simulation significantly.

Nevertheless, the linear relationship for the calibration curve on each day suggests that it is possible to run a small number of experiments to calibrate the noise strengths. Ideally, two experiments, one for a weak coupling case and the other for a strong coupling case, could be carried out and fitted to classical simulations to determine the noise characteristics. Note that accurate methods to simulate the dynamics in these two extremes are not as costly as simulating dynamics at the intermediate coupling regime [14], and therefore the HEOM method is not strictly required if a large system is under study. The relation can then be used to simulate dissipative dynamics under other system-bath coupling strengths by controlling only the damping coefficient on quantum computers. The fluctuation of noise strengths for the single-qubit decoherence-inducing gates is discussed in section S4 in the SI. Other methods to efficiently calibrate the noise strengths and, possibly, stabilize them are left for further research.

5. Concluding remarks

In this work, we have successfully simulated the EET dynamics for a symmetric dimer system under different damping regimes using only the intrinsic gate noises of the IBM-Q systems. Our approach requires neither additional ancillary qubits to represent the environment nor explicit bath engineering on the hardware level.

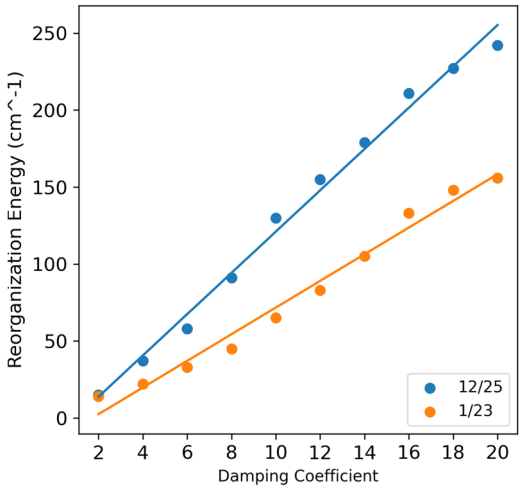

Figure 11. Calibration curves on different days. We plot the reorganization energy obtained from HEOM fitting against the damping coefficient used to generate quantum simulation data for experiments performed on different days. Blue dots denote results obtained on 2020/12/25, and yellow dots are results obtained on 2021/1/23. All experiments were performed on ibmq_paris.

Significantly, we show that by designing gate sequences to produce consistent random noises, the simulation scheme can yield results that are in excellent agreement with HEOM simulations of microscopic EET models. Moreover, although current superconducting quantum devices do not offer enough stability over time for consistent quantitative simulation of dissipative quantum dynamics, we show that a simple calibration scheme can be applied to turn NISQ devices into a controllable simulator for open quantum system dynamics to successfully predict the EET dynamics in the intermediate coupling regime.

It is also important to assess the scalability and the potential quantum advantage of the proposed simulation method. In principle, the decoherence-inducing gate method proposed here only needs N qubits to simulate the dissipative dynamics of a N-site system, and with superconducting quantum computers with more than 100 qubits readily available in the near future, it is possible to use our method to simulate large and complex excitonic systems such as the photosynthetic photosystem I (∼100 sites) and photosystem II supercomplex (∼300 sites), as well as conjugated polymers and a matrix of small-molecule chromophores used in organic solar cells. The realization of such simulations could significantly advance our understanding of elementary photophysical processes on these crucial systems. On the other hand, accurate classical simulation methods such as the HEOM approach demands significantly more computational cost and can not be easily applied to systems >100 sites. Generally speaking, with extremely efficient coding and parallel algorithmic optimization, the HEOM method could be applied to simulate a system with about 50 sites, but further scaling up would be formidable. Therefore, we present a quantum simulation algorithm that is highly likely to demonstrate clear quantum advantage in the near future. Nevertheless, current quantum hardware can only maintain coherence among a few nearest-neighbor qubits, which makes it difficult to carry out simulation beyond dimer systems. For bigger systems, additional error mitigation and calibration will be necessary for nowadays quantum hardware, and we are investigating in this direction.

Note that the advantages come naturally from using NISQ devices as a quantum noise generator, and our study indicates that the task is not trivial as nowadays NISQ devices could exhibit coherent noises that are not described by simple stochastic processes. The key insight in this work is that by choosing and designing specific compensating pulse sequences, purely random gate errors can be realized and controlled. Hence, intrinsic gate errors could and must be engineered to become a type of quantum resource. We believe that the major roadblock of the scheme proposed in this work remains the limited circuit depth available on nowadays NISQ devices.

We also noted that there exists a slight discrepancy between simulated dynamics and HEOM fitting at long time for the dynamics shown in figure 10(a), which can be attributed to accumulated errors in the deep quantum circuit needed to simulate long time dynamics. One possible method to remedy this inaccuracy in the long time dynamics is to use the transfer tensor algorithm [51] to tease out dynamical correlations in quantum simulation at the initial stage, and propagate the dynamic classically to an arbitrary long time. Such a hybrid quantum–classical approach would only need shallow quantum simulations and could make it possible to overcome the circuit depth problem. Of course, traditional transfer tensor algorithm needs dynamical map at each time step, and building up dynamical maps requires process tomography [52] on quantum computers. That makes the scaling not ideal for large systems. Thus, we envision that a more compact scheme to obtain dynamical maps

based on partial information of the underlying dynamics like compressed sensing techniques [53, 54] should be used if one is to extend the initial trajectories of the dissipative simulation of dynamics based on our scheme.

Our research also suggests a number of possible improvements. First of all, we only explored a controllable bath parameter that is the reorganization energies λ. It is important that a systematic procedure to adjust the cutoff frequencies γ can be found in order to generate baths with any desirable spectral properties. Presumably, dynamics with different γ can be simulated by designing different decoherence-inducing gates or by choosing a different unit-less energy scaling. Furthermore, additional research directions including detailed characterization of the effects of various decoherence-inducing gates, finer control over bath parameters using different gates or pulse level control (like pulse stretching), generating classically hard-to-simulate quantum noises, implementing finite temperature effect for biased exciton systems, and extending the simulations scheme to study larger systems with multiple sites could be foreseen to answer open questions with significant implications.

Interestingly, following the investigation of various decoherence-inducing gates, we also extract important characters of the gate noises. For example, we reveal that a large portion of $(X)^2$ gate errors consists of over-rotation. This 'off-set' type of error might not be as harmful as decoherent errors to quantum computers, because it could have been eliminated by more precise calibration of the pulses or adopting compensating pulse sequences like our design. However, conventional benchmark protocols only yield highly averaged metrics such as the average gate fidelity for the calibration of gate performance, which would provide limited information to properly describe the composition of the gate noises. Thus, we emphasize that the detailed characterization of the noises in current NISQ devices such as the analyses presented in the SI is still of vital importance for the design of error-mitigation or calibration protocols for quantum simulations.

Finally, we emphasize that the proposed decoherence-inducing gate sequences could serve as well-behaved quantum noise generator that may also be useful for other applications such as state preparation or dissipative quantum computation. We conclude that our results show the possibility of turning NISQ devices into extremely useful and programmable platforms to study open quantum systems under complicated system-bath interactions, and hopefully, can help us investigate complex dynamics in open quantum systems beyond what classical computers can do for us.

Acknowledgments

We thank IBM and IBM-Q Hub at NTU for accessing quantum devices through IBM Quantum Experience. YCC thanks the National Science and Technology Council, Taiwan (Grant No. NSTC 112-2119-M-002-018 and NSTC 111-2113-M-002-017), Physics Division, National Center for Theoretical Sciences (Grant No. 110-2124-M-002-012), and National Taiwan University (Grant No. 111L894603) for financial support.

Data availability statement

The data cannot be made publicly available upon publication because they contain commercially sensitive information. The data that support the findings of this study are available upon reasonable request from the authors.

Appendix. Experimental methods

Details on the encoding and propagation circuits and experimental setup on the IBM Q experience cloud service are provided as follows.

A.1. Encoding and propagating the exciton hamiltonian

To encode the Hamiltonian of the exciton dimer system in a quantum computer, a Jordan-Wigner type transformation [55] is used. There, the preparation step is trivial as the state preparation circuit for the exciton state with site 1 or 2 being excited can be easily implemented as shown in figure A1. Regarding mapping of the Hamiltonian, the second-quantized operators in (equation (1)) are mapped to the Pauli operators acting locally on qubits according to (equation (A1))

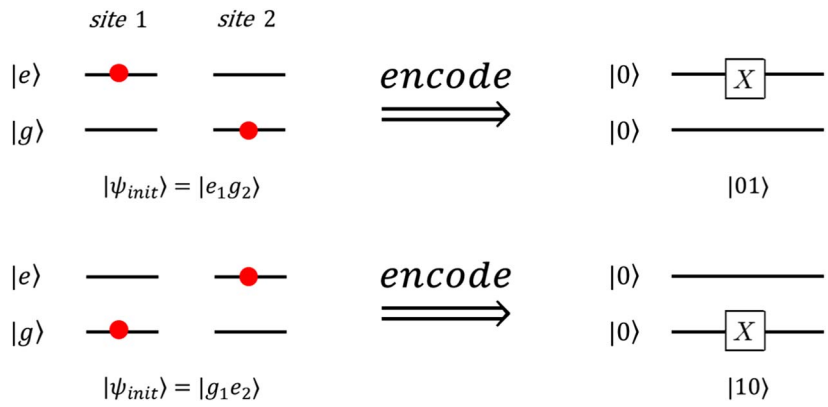

Figure A1. Encoding the exciton states in site basis on quantum computers The preparation of the initial state as $|1\rangle$ or $|2\rangle$ is implemented by applying an X gate to the corresponding qubit.

$$a_n^\dagger a_n = \frac{1}{2}(I_n - Z_n),$$
$$a_n^\dagger a_m + a_m^\dagger a_n = \frac{1}{2}(X_m X_n + Y_m Y_n),\ \forall\, m \neq n \tag{A1}$$

In our simulation, we model a symmetric dimer with $J_{12} = J_0$, therefore we can encode the unit-less $J = 1$ case without loss of generality. In this case, the simulation time has a derived unit of $1/J_0$. The qubit Hamiltonian can then be represented as

$$H = \frac{1}{2}(X_1 X_2 + Y_1 Y_2) \tag{A2}$$

To implement the time evolution operator e^{-iHt} on quantum computers ($\hbar = 1$), one can concatenate propagators for the local term. (figure 1(a)). The rotation angle θ of the phase gate $R_z(\theta)$ corresponds to the simulation time. In all our simulation of population dynamics, we set a single time step to be $\delta\theta = 0.03767$. (This corresponds to a step of 2 fs for a symmetric dimer system with excitonic coupling= 100 cm^{-1}). The decoherence period (ΔT_D) is chosen to be $25\delta\theta$, i.e. when d = 1, an identity gate sequence is prepended in the dissipation part for each 25 time steps.

A.2. IBM quantum experience

All the experiments are performed on superconducting quantum computers provided by IBM quantum experience [44] via qiskit framework [56]. Each job for the simulation of population dynamics consists of 150 circuits corresponding to evenly spaced simulation time. The logical-to-physical qubit mapping layout is chosen so that the CNOT interaction can be directly implemented. The qubit bit string is in little-endian format in accordance with the qiskit convention.

A.3. Population dynamics from projective measurements

To obtain the population in the site basis, we perform projective measurements up to 8192 times in qubit computational basis at each simulation time step, and calculate the population according to $P_1(t) = \frac{N_{01}(t)}{N_{01}(t)+N_{10}(t)}$. where N_{01}, and N_{10} are counts for the states collapsed to $|01\rangle$, $|10\rangle$, respectively. The counts for states collapsed to $|00\rangle$, $|11\rangle$ are excluded because they are generated by the leakage of population to space outside of the one-exciton manifold.

ORCID iDs

Shin Sun https://orcid.org/0009-0006-9491-7152

References

[1] Nielsen M A and Chuang I 2010 *Quantum Computation and Quantum Information* (Cambridge: Cambridge University Press) (https://doi.org/10.1017/CBO9780511976667)
[2] Bacon D, Childs A M, Chuang I L, Kempe J, Leung D W and Zhou X 2001 Universal simulation of markovian quantum dynamics *Phys. Rev.* A **64** 062302
[3] Georgescu I M, Ashhab S and Nori F 2014 Quantum simulation *Rev. Mod. Phys.* **86** 153
[4] Altman E *et al* 2021 Quantum simulators: Architectures and opportunities *PRX Quantum.* **2** 017003

[5] Yung M H, Whitfield J D, Boixo S, Tempel D G and Aspuru-Guzik A 2014 Introduction to quantum algorithms for physics and chemistry *Adv. Chem. Phys.* **154** 67–106
[6] O'Malley P J J *et al* 2016 Scalable quantum simulation of molecular energies *Phys. Rev. X* **6** 361–13
[7] Colless J I, Ramasesh V V, Dahlen D, Blok M S, Kimchi-Schwartz M E, McClean J R, Carter J, de Jong W A and Siddiqi I 2018 Computation of molecular spectra on a quantum processor with an error-resilient algorithm *Phys. Rev. X* **8** 011021
[8] Cao Y *et al* 2019 Quantum chemistry in the age of quantum computing *Chem. Rev.* **119** 10856–915
[9] McArdle S, Endo S, Aspuru-Guzik A, Benjamin S C and Yuan X 2020 Quantum computational chemistry *Rev. Mod. Phys.* **92** 015003
[10] Preskill J 2018 Quantum computing in the NISQ era and beyond *Quantum.* **2** 79
[11] Bharti K *et al* 2022 Noisy intermediate-scale quantum algorithms *Rev. Mod. Phys.* **94** 015004
[12] Knill E, Laflamme R and Zurek W H 1998 Resilient quantum computation *Science* **279** 342–5
[13] Bravyi S, Englbrecht M, König R and Peard N 2018 Correcting coherent errors with surface codes *npj Quantum. Inf.* **4** 55
[14] Breuer H-P *et al* 2002 *The theory of open quantum systems* (Oxford: Oxford University Press) (https://doi.org/10.1093/acprof:oso/9780199213900.001.0001)
[15] Ulrich W 2012 *Quantum Dissipative Systems* (London: World Scientific) (https://doi.org/10.1142/8334)
[16] Croce R and van Amerongen H 2020 Light harvesting in oxygenic photosynthesis: Structural biology meets spectroscopy *Science* **369** 933
[17] Arsenault E A, Yoneda Y, Iwai M, Niyogi K K and Fleming G R 2020 Vibronic mixing enables ultrafast energy flow in light-harvesting complex II *Nat. Commun.* **11** 1460
[18] Wang L, Allodi M A and Engel G S 2019 Quantum coherences reveal excited-state dynamics in biophysical systems *Nat. Rev. Chem.* **3** 477–90
[19] Rafiq S and Scholes G D 2019 From fundamental theories to quantum coherences in electron transfer *J. Am. Chem. Soc.* **141** 708–22
[20] Kim T W *et al* 2019 Ultrafast charge transfer coupled with lattice phonons in two-dimensional covalent organic frameworks *Nat. Commun.* **10** 1873
[21] Zurek W H 2003 Decoherence, einselection, and the quantum origins of the classical *Rev. Mod. Phys.* **75** 715
[22] Tanimura Y and Kubo R 1989 Time evolution of a quantum system in contact with a nearly Gaussian-Markoffian noise bath *J. Phys. Soc. Jpn.* **58** 101
[23] Tanimura Y 2006 Stochastic Liouville, Langevin, Fokker–Planck, and master equation approaches to quantum dissipative systems *J. Phys. Soc. Jpn.* **75** 082001
[24] Ishizaki A and Fleming G R 2009 Unified treatment of quantum coherent and incoherent hopping dynamics in electronic energy transfer: reduced hierarchy equation approach *J. Chem. Phys.* **130** 234111
[25] Jin J, Zheng X and Yan Y 2008 Exact dynamics of dissipative electronic systems and quantum transport: hierarchical equations of motion approach *J. Chem. Phys.* **128** 234703
[26] Mostame S, Rebentrost P, Eisfeld A, Kerman A J, Tsomokos D I and Aspuru-Guzik A 2012 Quantum simulator of an open quantum system using superconducting qubits: exciton transport in photosynthetic complexes *New J. Phys.* **14** 105013
[27] Trautmann N and Hauke P 2018 Trapped-ion quantum simulation of excitation transport: Disordered, noisy, and long-range connected quantum networks *Phys. Rev.* A **97** 023606
[28] García-Pérez G, Rossi M A C and Maniscalco S 2020 IBM Q Experience as a versatile experimental testbed for simulating open quantum systems *npj Quantum. Inf.* **6** 1
[29] Maniscalco S, Piilo J, Intravaia F, Petruccione F and Messina A 2004 F Intravaia, F Petruccione, and A Messina. Simulating quantum Brownian motion with single trapped ions *Phys. Rev.* A **69** 052101
[30] Chiuri A, Greganti C, Mazzola L, Paternostro M and Mataloni P 2012 Linear optics simulation of quantum non-markovian dynamics *Sci. Rep.* **2** 968
[31] Potočnik A *et al* 2018 Studying light-harvesting models with superconducting circuits *Nat. Commun.* **9** 904
[32] Wang B-X, Tao M-J, Ai Q, Xin T, Lambert N, Ruan D, Cheng Y-C, Nori F, Deng F-G and Long G-L 2018 Efficient quantum simulation of photosynthetic light harvesting *npj Quantum. Inf.* **4** 52
[33] Maier C, Brydges T, Jurcevic P, Trautmann N, Hempel C, Lanyon B P, Hauke P, Blatt R and Roos C F 2019 Environment-assisted quantum transport in a 10-qubit network *Phys. Rev. Lett.* **122** 050501
[34] Su H-Y and Li Y 2020 Quantum algorithm for the simulation of open-system dynamics and thermalization *Phys. Rev.* A **101** 012328
[35] Rost B, Jones B, Vyushkova M, Ali A, Cullip C, Vyushkov A and Nabrzyski J 2020 Simulation of thermal relaxation in spin chemistry systems on a quantum computer using inherent qubit decoherencearXiv:2001.00794
[36] Tolunay M, Liepuoniute I, Vyushkova M and Jones B A 2022 Hamiltonian simulation of quantum beats in radical pairs undergoing thermal relaxation on near-term quantum computersarXiv:2208.10107
[37] Guimarães J D, Lim J, Vasilevskiy M I, Huelga S F and Plenio M B 2023 Noise-assisted digital quantum simulation of open systemspsarXiv:2302.14592
[38] Feynman R P 1982 Simulating physics with computers *Int. J. Theor. Phys.* **21** 467–88
[39] Seth L 1996 Universal quantum simulators *Science* **273** 1073–8
[40] Klimov P V *et al* 2018 Fluctuations of energy-relaxation times in superconducting qubits *Phys. Rev. Lett.* **121** 090502
[41] Burnett J J, Bengtsson A, Scigliuzzo M, Niepce D, Kudra M, Delsing P and Bylander J 2019 Decoherence benchmarking of superconducting qubits *npj Quantum. Inf.* **5** 54
[42] Lieb E, Schultz T and Mattis D 1961 Two soluble models of an antiferromagnetic *chain. Ann. Phys.* **16** 407–66
[43] Low G H and Chuang I L 2017 Optimal hamiltonian simulation by quantum signal processing *Phys. Rev. Lett.* **118** 010501
[44] IBM quantum experience (https://quantum-computing.ibm.com/)
[45] Merrill J T and Brown K R 2014 Progress in compensating pulse sequences for quantum computation *Adv. Phys. Chem.* **154** 241–94
[46] Barreiro J T, Müller M, Schindler P, Nigg D, Monz T, Chwalla M, Hennrich M, Roos C F, Zoller P and Blatt R 2011 An open-system quantum simulator with trapped ions *Nature* **470** 486–91
[47] McKay D C, Wood C J, Sheldon S, Chow J M and Gambetta J M 2017 Efficient Z gates for quantum computing *Phys. Rev.* A **96** 022330
[48] Mohseni M, Rebentrost P, Lloyd S and Aspuru-Guzik A 2008 Environment-assisted quantum walks in photosynthetic energy transfer *J. Chem. Phys.* **129** 174106
[49] Chang H-T and Cheng Y C 2012 Coherent versus incoherent excitation energy transfer in molecular systems *J. Chem. Phys.* **137** 165103
[50] Strümpfer J and Schulten K 2012 Open quantum dynamics calculations with the hierarchy equations of motion on parallel computers *J. Chem. Theory Comput.* **8** 2808–16
[51] Cerrillo J and Cao J 2014 Non-Markovian dynamical maps: numerical processing of open quantum trajectories *Phys. Rev. Lett.* **112** 110401

[52] Mohseni M, Rezakhani A T and Lidar D A 2008 Quantum-process tomography: Resource analysis of different strategies *Phys. Rev.* A **77** 032322
[53] Gross D, Liu Y-K, Flammia S T, Becker S and Eisert J 2010 Quantum state tomography via compressed sensing *Phys. Rev. Lett.* **105** 150401
[54] Shabani A, Kosut R L, Mohseni M, Rabitz H, Broome M A, Almeida M P, Fedrizzi A and White A G 2011 Efficient measurement of quantum dynamics via compressive sensing *Phys. Rev. Lett.* **106** 100401
[55] Seeley J T, Richard M J and Love P J 2012 The Bravyi-Kitaev transformation for quantum computation of electronic structure *J. Chem. Phys.* **137** 224109
[56] Abraham H *et al* 2019 Qiskit: An open-source framework for quantum computing (https://doi.org.10.5281/zenodo.2562110)